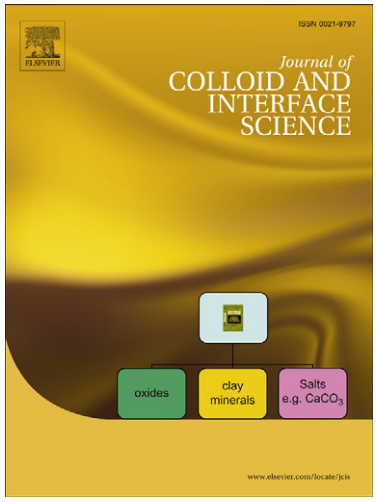

Kinetic and rheological measurements of the effects of inert 2-, 3- and 4-bromobenzoate ions on the cationic micellar-mediated rate of piperidinolysis of ionized phenyl salicylate

Nor Saadah M. Yusof, M. Niyaz Khan

PII: S0021-9797(11)00092-0
DOI: 10.1016/j.jcis.2011.01.061
Reference: YJCIS 16568

To appear in: *Journal of Colloid and Interface Science*

Received Date: 29 October 2010
Accepted Date: 20 January 2011

Please cite this article as: N.S.M. Yusof, M.N. Khan, Kinetic and rheological measurements of the effects of inert 2-, 3- and 4-bromobenzoate ions on the cationic micellar-mediated rate of piperidinolysis of ionized phenyl salicylate, *Journal of Colloid and Interface Science* (2011), doi: 10.1016/j.jcis.2011.01.061

Kinetic and rheological measurements of the effects of inert 2-, 3- and 4-bromobenzoate ions on the cationic micellar-mediated rate of piperidinolysis of ionized phenyl salicylate

Nor Saadah M. Yusof[a] and M. Niyaz Khan[a,*]

[a] *Department of Chemistry, Faculty of Science,University of Malaya, 50603 Kuala Lumpur, Malaysia*

[*] Corresponding author. Number: +6 03 7967 4163. Fax: +6 03 7967 4193

Email addresses: niyaz@um.edu.my, adah@um.edu.my

Abstract

The effects of the concentration of inert organic salts, [MX], (MX = 2-, 3- and 4-BrBzNa with 4-BrBzNa = 4-$BrC_6H_4CO_2Na$) on the rate of piperidinolysis of ionized phenyl salicylate (PS^-) have been rationalized in terms of pseudophase micellar (PM) coupled with an empirical equation. The appearance of induction concentration in the plots of k_{obs} versus [MX] (where k_{obs} is pseudo-first-order rate constants for the reaction of piperidine (Pip) with PS^-) is attributed to the occurrence of two or more than two independent ion exchange processes between different counterions at the cationic micellar surface. The derived kinetic equation, in terms of PM model coupled with an empirical equation, gives empirical parameters $F_{X/S}$ and $K_{X/S}$ whose magnitudes lead to the calculation of usual ion exchange constant K_X^{Br} (= K_X/K_{Br} with K_X and K_{Br} representing cationic micellar binding constants of counterions X^- and Br^-, respectively). The value of $F_{X/S}$ measures the fraction of S^- (= PS^-) ions transferred from the cationic micellar pseudophase to the aqueous phase by the optimum value of [MX] due to ion exchange X^-/S^-. Similarly, the value of $K_{X/S}$ measures the ability of X^- ions to expel S^- ions from cationic micellar pseudophase to aqueous phase through ion exchange X^-/S^-. This rather new technique gives the respective values of K_X^{Br} as 8.8 ± 0.3, 71 ± 6 and 62 ± 5 for X^- = 2-, 3- and 4-$BrBz^-$. Rheological measurements reveal the shear thinning behavior of all the surfactant solutions at 15 mM CTABr (cetyltrimethylammonium bromide) indicating indirectly the presence of rodlike micelles. The plots of shear viscosity (η) at a constant shear rate (γ), i.e. η_γ, versus [MX] at 15 mM CTABr exhibit maxima for MX = 3-BrBzNa and 4-BrBzNa while for MX = 2-BrBzNa, the viscosity maximum appears to be missing. Such viscosity maxima are generally formed in surfactant solutions containing long stiff and flexible rodlike micelles with entangled and branched/multiconnected networks. Thus, 15 mM CTABr solutions at different [MX] contain

long stiff and flexible rodlike micelles for MX = 3- and 4-BrBzNa and short rodlike micelles for MX = 2-BrBzNa.

Key Words: Kinetics of piperidinolysis of phenyl salicylate; Effects of organic salts and cationic micelles; Rheometric measurements; Counterionic ion exchange constants, K_X^{Br}; X = sodium 2-, 3-, and 4-bromobenzoates; Determination of K_X^{Br}.

1. Introduction

Aromatic organic anionic counterions such as salicylates [1,2], tosylates [3], mono- and disubstituted halobenzoates [2,4,5] as well as methylbenzoates [6,7] are among the most effective in promoting the cationic micellar growth. The apparent strong cationic micellar binding of these aromatic organic anionic counterions has been attributed to the presence of wormlike micelles [2,7,8]. This apparent and qualitative perception suggests the presence of a quantitative correlation between the magnitudes of the degree of counterion (X^-) binding (β_X) as well as cationic micellar binding constants of X^- (K_X) or ion exchange constants (K_X^{Br} where Br^- ion is a nonviscoelastic agent) and viscoelastic nature of X^-. The cationic micellar structural transition from spherical to rodlike micelles or vesicles has been found to accompany with significant increase in the values of β_X for X = Br^- [9-11]. But insignificant changes in β_X could be observed for aromatic counterions such as benzoate and substituted benzoate ions [12] 2-, 3- and 4-halobenzoates [13,14] as well as 2-, 3-, 4-methylbenzoates [14]. Thus, the cationic micellar structural transition with moderately hydrophobic counterions, such as benzoate (Bz^-), and substituted benzoate ions (W-Bz^-), could not be correlated accurately with β_X values of such cationic micelles [6,12-14].

Although the values of K_X^Y can be determined by the use of a variety of physicochemical techniques, the values of K_X^Y for Y = Br or Cl and X = benzoate, mono- and disubstituted benzoate ions could not be determined and consequently, the effects of these counterions on micellar growth were not quantified in any of the several such studies [2,6,12-15]. The values of K_X^Y for Y = Cl or OH, X = 2,6-dichlorobenzoate and various hydrophilic inorganic anions were found to be very technique-dependent [4 16]. A new semi-empirical kinetic technique has been used to determine the values of K_X^{Br} for X = 2-CH_3Bz^-, 3-CH_3Bz^- and 4-CH_3Bz^- of CTA^+ micellar system as 4 (5), 13 (12) and 12 [17] (9) [18], respectively. More than 2-fold stronger CTA^+ micellar affinity of 3-CH_3Bz^- and 4-CH_3Bz^- than that of 2-CH_3Bz^- explains qualitatively the rheological observations obtained previously [6]. The values of K_X^{Br} for X = 3- and 4-FBz^- and the effects of [MX] on CTABr micellar growth have been reported recently [19]. The values of K_X^{Br} for X = 2-$BrBz^-$, 3-$BrBz^-$ and 4-$BrBz^-$ are not available from literature. In the search for a quantitative correlation between the strength of counterion binding to CTABr micelles and the effects of the concentration of counterionic salts ([MX]) on CTABr micellar growth, the present study was aimed at (i) to use the new kinetic technique to determine the values of K_X^{Br} for MX = 2-, 3- and 4-BrBzNa at different values of $[CTABr]_T$ (total concentration of CTABr), and (ii) to carry out rheological measurements on aqueous solutions containing a constant value of [CTABr] and varying values of [MX]. The observed results and their probable explanations are described in this manuscript.

2. Materials and Methods

2.1 Materials.

Reagent-grade chemicals such as cetyltrimethylammonium bromide (CTABr), phenyl salicylate (PSL), 2-, 3- and 4-bromobenzoic acids (2-, 3- and 4-BrBzH) and piperidine (Pip) were commercial products of highest available purity. All other common chemicals used were also of reagent grade. The stock solutions (w M) of 2-, 3- and 4-$BrC_4H_6CO_2Na$ were prepared by adding (w + 0.05) M NaOH to the corresponding w M solutions of 2-, 3- and 4-BrBzH. The stock solution (0.01 M) of PSL was prepared in acetonitrile.

2.2 Methods

2.2.1 Kinetic Measurements. The kinetic measurements of the rate of nucleophilic substitution reaction between piperidine and ionized phenyl salicylate (PS^-) were carried out at 35 ^oC. The rate of disappearance of PS^- as a function of reaction time (t) was monitored spectrophotometrically at 350 nm. The details of the kinetic procedure and product characterization have been described elsewhere [17]. The absorbance values (A_{ob}) at different t were found to fit to equation 1 for ~ 8 half-lives of the reactions. All the symbols of

$$A_{ob} = [R_0]\, \delta_{ap} \exp(-k_{obs}\, t) + A_\infty \qquad (1)$$

equation 1, and the details of the data analysis are described in the recent report [19].

2.2.2 Rheological Measurements. The rheological study was carried out using Brookfield R/S+ rheometer with double gap coaxial cylinder (CC-DG) and the experimental details are the same as described earlier [19].

3. Results

3.1 Effects of the Concentrations of 2-, 3- and 4-$BrC_6H_4CO_2Na$ (2-, 3- and 4-BrBzNa) on k_{obs} for the Reaction of Pip with PS^- at a Constant $[CTABr]_T$.

Several kinetic runs were carried out at different concentrations of MX (= 2-BrBzNa or 3-BrBzNa or 4-BrBzNa) within [MX] range 0.0-0.50 M at a constant $[CTABr]_T$, 0.1 M piperidine (Pip) and 0.2 mM phenyl salicylate. The values of [NaOH] were varied from 0.03 to 0.055 M. Similar observations were obtained at different $[CTABr]_T$ within its range 5-15 mM at 35^{o}C. The values of pseudo-first-order rate constants (k_{obs}) at different [MX] are shown graphically in Figs. 1 and 2 for respective MX = 2- and 3-BrBzNa as well as Fig. 1 of "Supporting Materials" (SM) for MX = 4-BrBzNa. The calculated values of δ_{ap} were almost independent of [MX] within its range 0.0 - 0.50 M. The mean values of δ_{ap} (δ_{ap}^{avg}) at different $[CTABr]_T$ may be summarized as 10^{-1} δ_{ap}^{avg} = 725 ± 19, 715 ± 30, 729 ± 14, 715 ± 6 and 717 ± 13 $M^{-1}cm^{-1}$ for 2-BrBzNa; 697 ± 36, 701 ± 22, 688 ± 18, 695 ± 32 and 698 ± 17 $M^{-1}cm^{-1}$ for 3-BrBzNa; and 680 ± 20, 680 ± 20, 696 ± 19, 691 ± 15 and 685 ± 18 $M^{-1}cm^{-1}$ for 4-BrBzNa at 5, 6, 7, 10 and 15 mM CTABr, respectively.

3.2 Effects of the Concentrations of 2-, 3- and 4-BrBzNa on k_{obs} for the Reaction of Pip with PS^- at $[CTABr]_T$ = 0 and 35^{o}C.

Benzoate and substituted benzoate ions are nonreactive towards nucleophilic reaction with PS^-. But the inert salts of these ions may affect the rate constants for the nucleophilic substitution reaction of Pip with PS^- through salt/ionic strength effect. In order to find out the probable effects of such inert salts (MX = 2-, 3- and 4-BrBzNa) on k_{obs}, a few kinetic runs were carried out at 0.1 M Pip, 0.2 mM PS^- and within [MX] range 0.0 - ≤ 0.70 M. The concentration of NaOH was varied within the range 0.030 - ≤ 0.065 M. The calculated values of kinetic

parameters, k_{obs}, δ_{ap} and A_∞ at different [MX] (MX = 2-, 3- and 4-BrBzNa) are summarized in Table 1 of SM. The values of k_{obs} are almost independent of [MX] at ≤ 0.1 M for MX = 2-, 3- and 4-BrBzNa. A mild nonlinear decrease in k_{obs} with increasing values of [MX] at 0.1 M MX is evident from Table 1of SM.

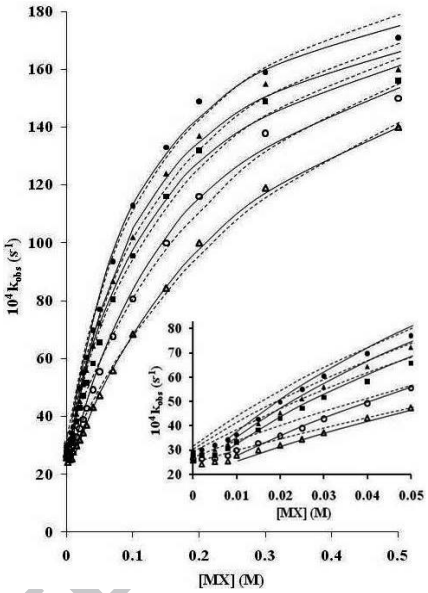

Fig. 1.

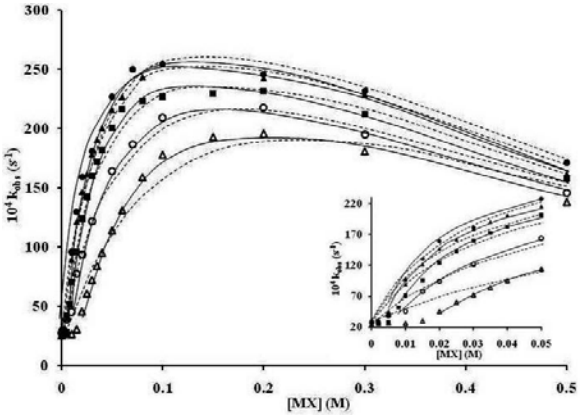

Fig. 2

3.3 Rheological Properties of Aqueous CTABr Surfactant Solutions Containing 0.2 mM PS^-, 0.1 M Pip, ≥ 30 mM NaOH, 15 mM CTABr and a Constant Value of [MX] (MX = 2-, 3- and 4-BrBzNa).

Rheological response of aqueous solution containing 0.2 mM PS^-, 0.1 M Pip, ≥ 30 mM NaOH, 15 mM CTABr, 2% v/v CH_3CN and a constant value of [MX] (MX = 2-BrBzNa or 3-BrBzNa or 4-BrBzNa) was studied at 33.2 ± 2.3 ^oC under steady-shear rate. The values of observed shear viscosity (η) as function of shear rate (γ), at constant [MX], are shown graphically as the log-log plots of Figs. 3 and 4 for MX = 2- and 4-BrBzNa, respectively as well as Fig. 2 of SM for MX = 3-BrBzNa. The ranges of [MX] were 20-400 and 5-100 mM for MX = 2- and 4-BrBzNa, respectively as well as 10-100 mM for MX = 3-BrBzNa. The plots of Figs. 3, 4 and Fig 2 of SM represent shear thinning which is a typical characteristic of aqueous surfactant solutions containing threadlike micelles [20-22].

The values of η at a constant γ (= 1.0 s^{-1}), i.e. $\eta_{1\gamma}$, [CTABr] (= 15 mM) and different [MX] are shown graphically in Fig. 5 for MX = 2-, 3- and 4-BrBzNa. An interesting and remarkable rheological feature of the plots of Fig. 5 is the presence of maxima. Although the presence of maxima in such plots is no longer unusual for viscoelastic/wormlike micellar systems [6,23-25], the mechanism, at the molecular level for the occurrence of such maximum is still a matter of uncertainty [8].

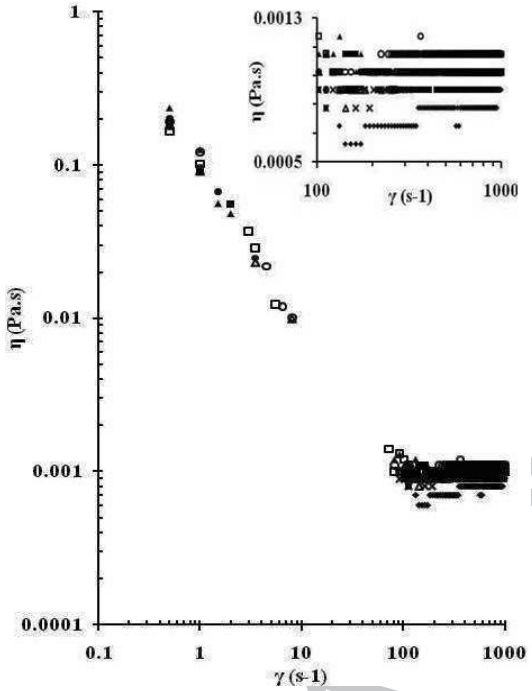

Fig. 3

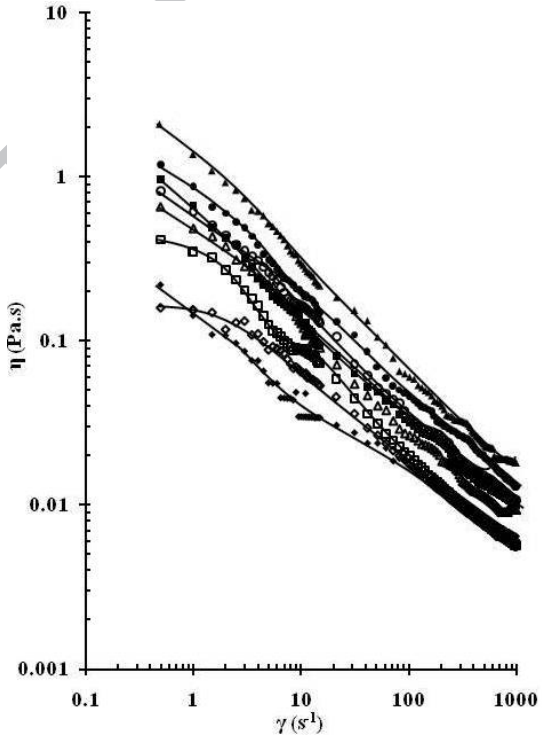

Fig. 4

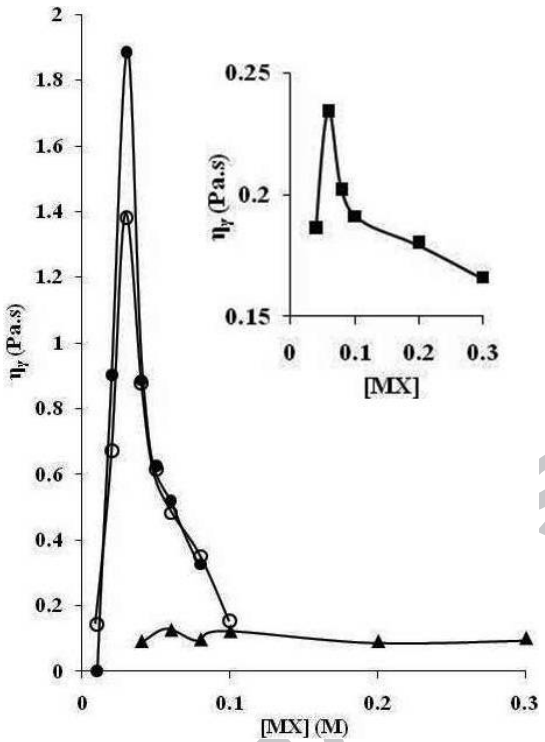

Fig. 5

4. Discussion

The reaction kinetic probe, that has been used in the present study for the determination of K_X^{Br} (ion exchange constant) for X = 2-, 3- and 4-$BrBz^-$, involves the effects of [MX] on k_{obs} for the reaction of Pip with PS^- at a constant concentration of CTABr micelles. The details of the following observations on this reaction kinetic probe have been described elsewhere [17,26]. (a) The products of the reaction of Pip with ionized phenyl salicylate (PS^-) are anionic N-piperidinylsalicylamide and phenol. (b) Phenyl salicylate molecules exist in ~100% ionized form (PS^-) under the experimental conditions of entire kinetic runs of present study. (c) The rates of uncatalyzed and hydroxide ion-catalyzed hydrolysis of PS^- are insignificant compared with the rate of piperidinolysis of PS^-. (d) The concentration of protonated piperidine ($[PipH^+]$) is

negligible compared with unprotonated piperidine ([Pip]) in the presence of 0.03-0.06 M NaOH and 0.0-0.015 M CTABr and consequently, $[Pip]_T \approx [Pip]$. This is also evident from the values of k_{obs} listed in Table 1 of SM. (e) The values k_{obs} at [MX] = 0 (Figs. 1, 2 and Fig. 1 of SM) are more than 10-fold smaller than k_{obs} for the reaction of Pip with PS^- at 0.1 M Pip and $[CTABr]_T$ = 0 (Table 1 of SM) [27,28]. The mechanistic details of CTABr micellar-mediated piperidinolysis of PS^- have been described elsewhere [27,29]. The observations (a)-(e) reveal a brief reaction scheme for the cleavage of PS^-, under the experimental conditions of the present study, as shown recently elsewhere [19].

The observed data listed in Table 1 of SM, show that the values of k_{obs} decreased by ≤ 3% with increase in [MX] from 0.0 to 0.10 M for MX = 2-, 3- and 4-BrBzNa. But the increase in [MX] from 0.0 to 0.50 M decreased k_{obs} by nearly 30, 80 and 60% for MX = 2-. 3- and 4-BrBzNa, respectively. The plots of Figs. 1,2 and Fig. 1 of SM show that the values of k_{obs} increase nonlinearly with the increase in [MX] until 0.50 M 2-BrBzNa and ≤ 15 mM CTABr, ~ 0.20 M 3- and 4-BrBzNa as well as ≤ 15 mM CTABr. The values of k_{obs} show a nonlinear decrease with the increase in [MX] at ≥ 0.1 M MX (where MX = 3-BrBzNa and 4-BrBzNa). The respective absence and presence of maxima in the plots of Fig. 1 and Fig. 2 as well as Fig. 1 of SM may be attributed to, at least, two factors, one that causes an increase in k_{obs} with increasing [MX] and second is a negative salt effect (as evident from Table 1 of SM). Significantly weaker negative salt effect for 2-BrBzNa than those for 3- and 4-BrBzNa may be attributed to the absence of maxima in the plots of Fig. 1. Perhaps it is noteworthy that the presence of maxima was not observed in the plots of k_{obs} versus [MX] at ≤ 0.3 M MX and ≤ 15 mM CTABr for MX = 3- and 4-FBzNa [19].

The nonlinear increase in k_{obs} with increasing values of [MX] at a constant value of $[CTABr]_T$ cannot be explained in terms of ionic strength or specific ion effect (Table 1 of SM). The anions X^- (= 2-, 3- and 4-$BrBz^-$) are extremely weak nucleophiles and hence they cannot be expected to react with PS^-. Furthermore, a nucleophile must contain, at least, one hydrogen atom attached to its nucleophilic site in order to become an efficient reactive nucleophile for its nucleophilic reactivity towards PS^- because of the occurrence of intramolecular general base assistance in such reactions [30]. Since the rate of piperidinolysis of PS^- is > 10-fold larger in aqueous phase than that in CTABr micellar pseudophase, it is obvious that the most likely source for the nonlinear increase in k_{obs} with the increase in [MX] (Figs. 1,2 and Fig. 1 of SM) is the transfer of micellized PS^- (i.e. PS^-_M) to the aqueous phase through the ion exchange process X^-/PS^-.

The values of k_{obs} at different [MX] and at constant values of $[CTABr]_T$, were treated with equation 2

$$k_{obs} = \frac{k_0 + \theta K^{X/S}[MX]}{1 + K^{X/S}[MX]} \qquad (2)$$

where θ and $K^{X/S}$ are empirical constant and $k_0 = k_{obs}$ at [MX] = 0 and [micelles] $\neq$ 0. The effects of the concentration of various inert inorganic and organic salts on k_{obs} for alkaline hydrolysis and aminolysis of phthalimide, PS^-, phenyl benzoate and *N*-benzylphthalimide, at constant [cationic micelles], [amine nucleophile] and [NaOH], have been explained satisfactorily (in terms of, at least, residual errors) by the use of equation 2 [31]. The nonlinear least-squares technique was used to calculate the values of θ and $K^{X/S}$ as well as least-squares, $\sum di^2$, from

equation 2 by considering k_0 as a known parameter. The values of k_0 were obtained experimentally at [MX] = 0 and under the rest of the reaction conditions of the kinetic runs where [MX] ≠ 0. The least-squares calculated values of θ, $K^{X/S}$ and $\sum di^2$ at different $[CTABr]_T$ for MX = 2-BrBzNa are summarized in Table 1. The extent of the reliability of the observed data fit to equation 2 is evident from the plots of Fig. 1 where dashed lines are drawn through the calculated rate constants using equation 2 with calculated parameters (θ and $K^{X/S}$) shown in Table 1. The standard deviations associated with θ and $K^{X/S}$ values also reflect the quality of the observed data fit to equation 2.

Table 1

It is apparent from equation 2 that the values of k_{obs} should be independent of [MX] under the limiting conditions where $\theta K^{X/S}[MX] >> k_0$ and $K^{X/S}[MX] >> 1$ provided k_{obs} values are independent of [MX] at $[CTABr]_T = 0$. But the values of k_{obs} of Table 1 of SM show nearly 30, 80 and 60% decrease with the increase in [MX] from 0.0 to 0.50 M for respective MX = 2-, 3- and 4-BrBzNa. Because of the presence of significant negative salt effect for 3- and 4-BrBzNa on k_{obs}, the data treatment for these two salts was carried out with equation 2 by the replacement of θ with $F_{X/S}\, k_{obs}^{MX}$ where $F_{X/S}$ represents an empirical constant whose magnitude should be in the range ≤ 1.0 - > 0 and $k_{obs}^{MX} = k_{obs}$ at a typical value of [MX] and $[CTABr]_T = 0$ (Table 1 of SM). The nonlinear least-squares calculated values of $F_{X/S}$, $K^{X/S}$ and $\sum di^2$ at different $[CTABr]_T$ are summarized in Table 1 for MX = 3-BrBzNa and 4-BrBzNa. The calculated values of $F_{X/S}$ are not appreciably different from 1.0 at different values of $[CTABr]_T$ (Table 1) which support the perception that the downturn curvatures of the plots of Fig. 2 and Fig. 1 of SM are due to merely negative salt effect on k_{obs}. The extent of satisfactory observed data fit to equation 2 (where θ =

$F_{X/S}\ k_{obs}^{MX}$) is evident from the plots of Fig. 2 and Fig. 1 of SM where dashed lines are drawn through calculated rate constants using equation 2 and calculated parameters ($F_{X/S}$ and $K^{X/S}$) summarized in Table 1.

The dashed line plots of Figs. 1,2 and Fig. 1 of SM display significant systematic negative deviations of the observed data points from the corresponding predicted data points of dashed lines at the lower values of [MX]. The absolute magnitudes of these negative deviations increase with the decrease in [MX] as well as increase in $[CTABr]_T$. Such observations, in the related studies [18,19], have been attributed to the effects of the occurrence of independent ion exchange processes X^-/HO^- and X^-/Br. The occurrence of these ion exchange processes (X^-/HO^- and X^-/Br^-) is expected to decrease the effective concentration of [MX] ($[MX]_S^{ef}$) affecting the ion exchange process X^-/S^- (where S^- = PS^-). As described elsewhere [18,19], the value of $[MX]_S^{ef}$ is related to [MX] through the following relationships:

$$[MX]_S^{ef} = [MX] - [MX]_0^{op} \qquad (3)$$

where $[MX]_0^{op} = [MX]_{OH}^{op} + [MX]_{Br}^{op}$ with $[MX]_{OH}^{op}$ and $[MX]_{Br}^{op}$ representing the optimum values of [MX] at which a further increase in [MX] has no effect on ion exchange X^-/HO^- and X^-/Br^-, respectively.

The values of $[MX]_0^{op}$, at different $[CTABr]_T$, were calculated by an iterative technique [19]. These calculated values of $[MX]_0^{op}$, at different $[CTABr]_T$, are summarized in Table 1 for MX = 2-, 3- and 4-BrBzNa. The values of $[MX]_0^{op}$ show the increase of ~ 0.5-, 3.0- and 3.0-fold with the increase in $[CTABr]_T$ from 5.0 to 15 mM for 2-, 3- and 4-BrBzNa, respectively. The nonlinear least-squares calculated values of θ, $K^{X/S}$ and $\sum di^2$ for 2-BrBzNa as well as $F_{X/S}$, $K^{X/S}$

and $\sum di^2$ for 3- and 4-BrBzNa by the use of equation 2 (with the replacement of [MX] with $[MX]_S^{ef}$) are also listed in Table 1. It is evident from the plots of Figs. 1,2 and Fig. 1 of SM, where the solid lines are drawn through the calculated data points using equation 2 (by the replacement of θ with $F_{X/S}\, k_{obs}^{MX}$ for 3- and 4-BrBzNa), as well as from the values of $\sum di^2$ that the data treatment with equation 2 is more reliable with [MX] = $[MX]_S^{ef}$ at $[MX]_0^{op} \neq 0$ compared with that at $[MX]_0^{op} = 0$.

4.1 Effects of Pure CTABr Micelles on the Kinetic Data Obtained at a Constant [MX]. The values of k_{obs}, obtained under such conditions, are expected to follow equation 4 which is derived based upon the pseudophase micellar (PM) model [32,33].The symbols of equation 4 are explained elsewhere [19].

$$k_{obs} = \frac{k^n_W + k^{mr}_M K_N K_S [D_n] [Pip]_T}{1 + K_S [D_n]} \quad (4)$$

The effective occurrence of ion exchange process X^-/S^-, in the related reaction systems, has been found to decrease K_S with the increase of [MX] through an empirical relationship (equation 5)

$$K_S = K_S^0 / (1 + K_{X/S} [MX]) \quad (5)$$

where $K_S^0 = K_S$ at [MX] = 0 [27,34]. The magnitude of the empirical constant, $K_{X/S}$ (equation 5) is the measure of the ability of counterion, X^-, to expel another counterion, S^-, from the cationic micellar pseudophase to the aqueous phase through the occurrence of ion exchange process X^-/S^- at the cationic micellar surface. Equations 4 and 5 can lead to equation 2 with k_0, θ and $K^{X/S}$ given by respective equations 6, 7 and 8,

$$k_0 = \frac{k_W + k^{mr}_M K_N K_S^0 [Pip]_T [D_n]}{1 + K_S^0 [D_n]} \quad (6)$$

where $k_W = k_{obs}$ ($= k^n_W [Pip]_T$) at $[D_n] = [MX] = 0$ as well as K_N is assumed to be independent of [MX],

$$\theta = F_{X/S} k^n{}_W{}^{MX} [Pip]_T \quad (7)$$

where $k^n{}_W{}^{MX} [Pip]_T = k_{obs}$ at a typical value of [MX] and $[D_n] = 0$ as well as $F_{X/S}$ is an empirical constant whose value should be (by definition) in the range > 0 - ≤ 1.0, and

$$K^{X/S} = \frac{K_{X/S}}{1 + K_S^0 [D_n]} \quad (8)$$

where $[D_n] \approx [CTABr]_T$ under the experimental conditions of this study [19].

The reason for the appearance of $F_{X/S}$ in equation 7 is described in detail elsewhere [35]. It has been also concluded in the earlier report [35] that, under the present experimental conditions, the values of $F_{X/S}$ should measure (i) the fraction of the micellized counterions, S^- (i.e. S^-_M) transferred to aqueous phase by the limiting value of [MX] due to ion exchange X^-/S^- and (ii) the cationic micellar penetration of X^- compared with that of S^-.

In view of equation 7, the values of θ or $F_{X/S}$ should be independent of $[D_n]$ or $[CTABr]_T$. The values of θ for 2-BrBzNa and $F_{X/S}$ for 3-BrBzNa and 4-BrBzNa (Table 1) appear to be in agreement with this prediction. The values $F_{X/S}$ for 2-BrBzNa at different $[CTABr]_T$ were calculated from equation 7 with $k^n_W = 0.327\ M^{-1}s^{-1}$ [19] and $[Pip]_T = 0.1$ M and these results are summarized in Table 1. The mean values of $F_{X/S}$ for 2-, 3- and 4-$BrBz^-$ are shown in Table 2. The more reliable mean values of $F_{X/S}$ (obtained at $[MX]_0^{op} \neq 0$) reveal that the CTABr micellar

penetration of 2-$BrBz^-$ ($F_{X/S}$ = 0.63) is significantly lower than those for 3-$BrBz^-$ ($F_{X/S}$ = 0.92) and 4-$BrBz^-$ ($F_{X/S}$ = 0.99). It may be noted that the micellar penetration of these substituted benzoate anions does not mean that these ions enter the hydrophobic core of the micelles where water concentration is nearly zero. The values of $F_{X/S}$ for X = 3- and 4-$BrBz^-$ are lager (by ~ 20%) than those X = 3- and 4-FBz^- [19], respectively. The value of $F_{X/S}$ is expected to be governed by the hydrophobicity/hydrophilicity balance of counterion X^- [36]. The electronegativity and polarizability of F, Cl, Br and I as well as hydrophilicity and hydrophobicity of micellar pseudophase vary in the opposite direction. Similarly, the effects of polarity/steric requirements and polarizability of counterions on their ionic micellar penetration are expected to oppose each other. These characteristics of substituted benzoate counterions and cationic micellar pseudophase determine the extent of the micellar penetration of counterions i.e. the values of $F_{X/S}$.

The values of $K_{X/S}$ at different $[CTABr]_T$ were calculated from equation 8 with $K_S^0 = 7.0 \times 10^3$ M^{-1} [31,37] and $[D_n] \approx [CTABr]_T$ under the experimental conditions of this study. These calculated values of K_X^{Br} for X = 2-, 3- and 4-$BrBz^-$ are summarized in Table 1. These values of K_X^{Br} are almost independent of $[CTABr]_T$ within its range 5-15 mM (Table 1) and the mean values of K_X^{Br} for X = 2-, 3- and 4-$BrBz^-$ are shown in Table 2. As described in some details elsewhere, [19] the empirical definitions of $K_{X/S}$ and $F_{X/S}$ can lead to equation 9

$$\frac{K_{X/S}^n}{K_{Y/S}^n} = \frac{K_X}{K_Y} \qquad (9)$$

where $K_X/K_Y = K_X^Y = ([X_M][Y_W])/([X_W][Y_M])$ with K_X and K_Y representing respective ionic micellar binding constant of counterions X and Y, $K_{X/S}^n = F_{X/S} K_{X/S}$, $K_{Y/S}^n = F_{Y/S} K_{Y/S}$ and S, Y

and X represent counterions of ionic micelles (i.e. CTA^+ surfactants). The calculated values of $K_{X/S}^n$ (= $F_{X/S}$ $K_{X/S}$, Table 1) and the reported value of 25 M^{-1} [19,35] for $K_{Br/S}^n$ with $S = S^-$ (i.e. PS^-) give the values of K_X^{Br} (by the use of equation 9 with Y = Br) for different counterions X. These calculated values of K_X^{Br} for X = 2-, 3- and 4-$BrBz^-$ at different $[CTABr]_T$ are also shown in Table 1. The values of K_X^{Br} are almost independent of [CTABr] for a typical X ion (Table 1). The mean values of K_X^{Br} for X = 2-, 3- and 4-$BrBz^-$ are summarized in Table 2.

Table 2

The value of K_X^{Br} (= 8.8) for X = 2-$BrBz^-$ is 8- and 7- fold smaller than K_X^{Br} for X = 3- and 4-$BrBz^-$, respectively. These results may be attributed to the orientational effect of substituent Br in the benzene ring of Bz^-. Almost similar results were obtained with X = 2- and 3-$ClBz^-$ [39,40]. The value of K_X^{Br} for X = 2-$BrBz^-$ is ~ 2-fold larger than that for X = 2-$ClBz^-$ which could be ascribed to a few factors including electronegativity and polarizability effects of Cl and Br.

The values of $[MX]_0^{op}$ show a nonlinear increase with the increase of $[CTABr]_T$ from 5 to 15 mM (Table 1). The values of this increase are 1.5, 4.0- and 4.0-fold for MX = 2-, 3- and 4-BrBzNa, respectively. These results are plausible in view of 8- to 7-fold larger values of K_X^{Br} for X = 3- and 4-$BrBz^-$ than that for X = 2-$BrBz^-$. Significantly low increase (~ 2- to 3-fold) of $[MX]_0^{op}$ with increasing values of $[CTABr]_T$ from 5 to 15 mM for MX = 3- and 4-FBzNa [19] is attributed to ~ 5-fold smaller values of K_X^{Br} for X = 3- and 4-FBz^- than those for X = 3- and 4-$BrBz^-$.

4.2 Rheological Behavior of 15 mM CTABr Aqueous Solutions Containing 2-, 3- and 4-BrBzNa.

Generally, shear viscosity (η) versus shear rate (γ) plot of viscoelastic micellar system reveals four distinct regions, i.e. Newtonian, shear thinning, shear thickening and shear thinning [7]. However, in various studies on viscoelastic surfactant solutions, shear thickening regions in the plots of η versus γ have not been observed [41-43]. It has been suggested that in some of these studies, it is possible that an SIS together with a second shear thinning region might appear at $\gamma > 1000\ s^{-1}$ [7]. The expected first Newtonian region is completely missing in the plots of Fig. 3 and it is not very clear in the plots of Fig. 4 and Fig. 2 of SM. Generally, the first Newtonian region appears at very low shear rate ($< 0.2\ s^{-1}$). The rheometer, used in this study, could not detect the shear viscosity at such low shear rates in the presence of varying concentration of 2-, 3- and 4-$BrBz^-$ at 15 mM CTABr. The plots of Fig. 3 do not show the presence of SIS regions and as a consequence, second shear thinning regions are also absent. Although the plots of Fig. 4 and Fig. 2 of SM do not reveal the presence of SIS regions, some of these plots (such as those at 0.03, 0.04, 0.06 and 0.08 M 3-BrBzNa of Fig. 4 and 0.01-0.08 M 4-BrBzNa of Fig. 2 of SM) do show the presence of two different shear thinning segments/regions. The nature and shape of the plots of Fig. 3 are very different compared to those of Fig. 4 and Fig. 2 of SM and this distinctive difference may be attributed to ≥ 7-fold larger values of K_X^{Br} for X = 3-$BrBz^-$ and 4-$BrBz^-$ than that for X = 2-$BrBz^-$.

Viscoelastic/wormlike ionic micellar solutions have been found to generally exhibit the nonlinear plots of η_γ versus [MX] with at least, a well defined maximum in each such plot where η_γ and [MX] represent shear viscosity at a constant shear rate (γ) and counterionic salt concentration, respectively [6,23-25]. In view of these reports, the viscosity maxima plots of Fig. 5 reveal that 15 mM CTABr solutions, containing varying values of [3-BrBzNa] (0.03 – 0.1 M) and [4-BrBzNa] (range 0.005 – 0.1 M) contain wormlike micelles. Cryo-TEM image of aqueous

CTACl/4-BrBzNa system containing 5 mM CTACl and 20 mM 4-BrBzNa reveals the presence of long stiff and less entangled threadlike micelles (i.e. larger persistence length compared with CTACl/4-IBzNa system) [13]. The aqueous solutions of CTACl/4-BrBzNa at 5 mM CTACl and within [4-BrBzNa] range 3-20 mM exhibited both drag reduction and viscoelastic properties [13]. The maxima of the plots of Fig. 5 occur at $[MX]/[CTABr]_T$ (R_s) ≈ 3.3 for MX = 3-BrBzNa and R_s ≈ 2.7 for MX = 4-BrBzNa. The shape of the plots of Fig. 5 remained essentially unchanged while R_s values changed from ~ 3.3 to ~ 2.7 (for MX = 3-BrBzNa) and from ~ 2.7 to ~ 2.0 (for MX = 4-BrBzNa) with the increase in γ value from 1.0 to 152 s^{-1}.

The plot of $\eta_{1\gamma}$ versus [2-BrBzNa] (Fig. 5) does not appear to have a well defined maximum and as a consequence the presence of wormlike micelles in 15 mM CTABr solutions containing varying values of [2-BrBzNa] (range 0.02 – 0.4 M) is highly unlikely. However, the plots of Fig. 3 rule out the presence of spherical micelles at > 0.04 M 2-BrBzNa because these plots represent surfactant solutions as non-Newtonian fluid system. In view of these observations, it appears that aqueous solutions containing 15 mM CTABr and ≥ 0.04 M 2-BrBzNa contain short and stiff linear rodlike micelles. This conclusion is supported by the conductivity measurements of tetradecyltrimethylammonium surfactants comicellized with 2-$BrBz^-$ where the presence of rodlike micelles has been proposed [14].

It has been a general perception, although based upon merely qualitative observations, that the specific and strong counterions binding to ionic micelles cause micellar growth from short rodlike to long stiff and flexible rodlike/wormlike to entangled and branched/multiconnected micelles [2,7,8,44,45]. The values of K_X^{Br} for X = Bz^-, 2-CH_3Bz^-, 2-$ClBz^-$ and 2,6-Cl_2Bz^- are ~ 5 (Table 2) and these counterions of CTA^+ micelles are known to

produce only spherical micelles at ≤ 20 mM CTABr [4,5]. On the other hand, counterionic salts (MX), such as 3-ClBzNa, 4-ClBzNa and 4-BrBzNa, induce the formation of long linear and branched wormlike micelles at ≤ 20 mM MX and 5 mM CTACl [5,13]. But the counterionic salt 4-FBz^- could produce only spherical and some short rodlike micelles at ≤ 20 mM MX and 5 mM CTACl [5,13]. Rheometric measurements exhibited the presence of long wormlike micelles at 50 mM CPyCl and > ~ 40 mM MX with MX = 3-CH_3BzNa and 4-CH_3BzNa [6]. The more reliable values of K_X^{Br} for X = 2-$BrBz^-$, 3-$BrBz^-$, 4-$BrBz^-$, 3-FBz^-, 4-FBz^-, 3-$ClBz^-$, 3-CH_3Bz^- and 4-CH_3Bz^- (Table 2) reveal a rather quantitative correlation between the magnitudes of K_X^{Br} and the ability of X^- to induce the formation of short rodlike, long stiff and flexible rodlike/wormlike as well as entangled and branched/multiconnected micelles under a specific and comparable conditions (in terms of the concentrations of cationic surfactant(s) and MX).

The value of the specific concentration of MX (= $[MX]_{sc}$) at which viscosity maximum occurred in the plot of η_γ versus [MX] is ~ 40% lower for MX = 3- and 4- BrBzNa than that for MX = 3- and 4- FBzNa (Table 2). These results reveal that the increase in K_X^{Br} value decreases the value of $[MX]_{sc}$ at a constant $[CTABr]_T$ which is plausible if the perception that, at a constant [ionic surfactant], the counterionic salt (MX)-induced micellar structural transition from sphere - rodlike (of increasing lengths – stiff – flexible) depends upon the magnitudes of ionic micellar binding constants (K_X) of counterions X.

5. Conclusions

The new and perhaps interesting aspects of the present manuscript are the experimentally evaluated magnitudes of K_X^{Br} and $F_{X/S}$ for X = 2-,3- and 4-$BrBz^-$. The values of K_X^{Br} are 9, 71 and 62 for X = 2-, 3- and 4- $BrBz^-$, respectively. Rheometric measurements reveal the presence

of short rodlike and long linear and entangled rodlike micelles in aqueous solutions of 15 mM CTABr/MX for MX = 2-BrBzNa and 3-, 4- BrBzNa, respectively. The notable feature of these observations is that, perhaps for the first time, a quantitative correlation between counterionic (X^-) affinity (measured by the value of K_X^{Br}) of CTABr micelles and the [X^-]–induced micellar structural growth from spherical to short and long rodlike micelles has been achieved. The values K_X^{Br} for X = 3- and 4-FBz^- are ~ 5-fold [19] lower than those for X = 3- and 4-$BrBz^-$ and these observations correlate well with cryo-TEM images of 5 mM CTACl/20 mM MX containing mixed more spherical + less long rodlike micelles for MX = 4-FBzNa and stiff long as well as less entangled rodlike micelles for for MX = 4-BrBzNa [13]. The kinetic validity of equation 3 constitutes the indirect evidence for the occurrence of two or more than two independent ion exchange processes at the cationic micellar surface. The values of $[MX]_{sc}$ decreases with increasing values of K_X^{Br} for X =3-, 4-FBz^- [19] and 3-, 4-$BrBz^-$ (Table 2) at 15 mM CTABr. Similar observations were observed in a recent related study [15].

Acknowledgements

The authors thank the University of Malaya (UM) for financial assistance through research grant RG022/09AFR, and the Centre of Ionic Liquids, UM for the permission to carry out the rheological study.

References

[1] A. Shukla and H. Rehage, Langmuir, 24 (2008)**,** 8507.

[2] U. R. K. Rao, C. Manohar, B. S. Valaulikar, and R. M. Iyer, J. Phys. Chem., 91 (1987), 3286.

[3] B. A. Schubert, E. W. Kaler, and N. J. Wagner, Langmuir, 19 (2003) 4079.

[4] L. J. Magid, Z. Han, G. G. Warr, M. A. Cassidy, P. D. Butler, and W. A. Hamilton, J. Phys. Chem. B, 101 (1997), 7919.

[5] B. Lu, X. Li, L. E. Scriven, H. T. Davis, Y. Talmon, and L. J. Zakin, Langmuir, 14 (1998) 8.

[6] H. Rehage and H. Hoffmann, Molecular Phys., 74 (1991) 933 and references therein.

[7] Y. Qi, and J. L. Zakin, Ind. Eng. Chem. Res., 41 (2002), 6326.

[8] T. S. Davies, A. M. Ketner, and S. R. Raghavan, J. Am. Chem. Soc., 128 (2006) 6669.

[9] Y. Geng, L. S. Romsted and F. Menger, J. Am. Chem. Soc., 128 (2006), 492.

[10] Y. Ono, H. Kawasaki, M. Annaka and H. Maeda, J. Colloid Interface Sci, 287 (2005) 685.

[11] A. Rodriguez, M. M. Graciani, F. Cordobes and M. L. Moya, J. Phys. Chem. B, 113 (2009) 7767.

[12] J. Penfold, I. Tucker, E. Staples and R. K. Thomas, Langmuir, 20 (2004) 8054.

[13] W. Ge, E. Kesselman, Y. Talmon, D. J. Hart and J. L. Zakin, J. Non-Newtonian Fluid Mech., 154 (2008) 1.

[14] M. Vermuthen, P. Stiles, S. J. Bachofer and U. Simonis, Langmuir, 18 (2002) 1030.

[15] C. Oelschlaeger, P. Suwita, N. Willenbacher, Langmuir, 26 (2010) 7045.

[16] L. S. Romsted, Micellar effects on reaction rates and equilibria, in: K. L. Mittal, B. Lindman (Eds.), Surfactant in Solutions, vol. 2, Plenum, New York, 1984, pp. 1015-1068.

[17] M. N. Khan and S. Y. Kun, J. Chem Soc Perkin Trans 2, (2001) 1325 and references therein.

[18] M. N. Khan and E. Ismail, J. Mol. Liq., 136 (2007) 54.

[19] N. S. M. Yusof and M. N. Khan, Langmuir , 26 (2010) 10627.

[20] T. Lu, J. Huang, Z. Li, S. Jia and H. Fu, J. Phys. Chem. B, 112 (2008) 2909.

[21] S. R. Raghavan and E. W. Kaler, Langmuir, 17 (2001) 300 and references therein.

[22] Y. Lin, X. Han, J. Huang, H. Fu and C. Yu, J. Colloid Interface Sci., 330 (2009) 449.

[23] H. Rehage and H. Hoffmann, J. Phys. Chem., 92 (1988) 4712.

[24] C. A. Dreiss, Soft Matter, 3 (2007) 956 and references therein.

[25] B. Dong, A. Zhang, L. Zheng, S. Wang, X. Li and T. J., J. Colloid Interface Sci., 319 (2008) 338.

[26] M. N. Khan and E. Ismail, Indian J. Chem., 48A (2009) 781 and references therein.

[27] M. N. Khan, Z. Ariffin, E. Ismail and S. F. M. Ali, J. Org. Chem., 65 (2000) 1331.

[28] M. N. Khan and E. Ismail, Prog. Reaction Kinet. Mech., 31 (2006) 205.

[29] M. N. Khan, Z. Ariffin, M. N. Lasidek, M. A. M. Hanifiah and G. Alex, Langmuir, 13 (1997) 3959.

[30] M. N. Khan, J. Phys. Chem., 92 (1988) 6273.

[31] M. N. Khan, Micellar Catalysis. In Surfactant Science Series; CRC Press; Taylor & Francis Group. Boca Raton, FL, 2006: vol. 133, chap. 3.

[32] C. A. Bunton and G. Savelli, Adv. Phys. Org. Chem., 22 (1986) 213.

[33] C. A. Bunton, F. Nome, F. Quina, L. S. Romsted, Acc. Chem. Res., 24 (1991) 357 and references therein.

[34] M. N. Khan, J. Org. Chem., 62 (1997) 3190.

[35] M. N. Khan, Adv. Colloid Interface Sci., 159 (2010) 160.

[36] V. Subramaniam and W. A. Ducker, Langmuir, 16 (2000) 4447.

[37] M. N. Khan, Z. Arifin, I. A. Wahab, S. F. M. Ali and E. Ismail, *Colloids Surf. A, 163 (***2000**) 271.

[38] M. N. Khan and E. Ismail, J. Dispersion Sci. Technol., 31 (2010) 314.

[39] M. N. Khan and R. Yusoff, J. Phys. Org. Chem., 14 (2001) 74.

[40] M. N. Khan and E. Ismail, J. Phys. Chem. A, 113 (2009) 6484 and references therein.

[41] B. A. Schubert, J. W. Wagner, E. W. Kaler and S. R. Raghavan, Langmuir, 20 (2004) 3564.

[42] B. A. Schubert, E. W. Kaler and N. J. Wagner, Langmuir, 19 (2003) 4079.

[43] V. Croce, T. Cosgrove, C. A. Dreiss, S. King, G. Maitland and T. Hughes, T., Langmuir 21 (2005) 6762.

[44] L. Ziserman, L. Abezgauz, O. Ramon, S. R. Raghavan and D. Danino, Langmuir, 25 (2009) 10483.

[45] C. Oelschlaeger, M. Schopferer, F. Scheffold and N. Willenbacher, Langmuir, 25 (2009) 716.

Fig. 1. Plots showing the dependence of k_{obs} upon [MX] (MX = 2-BrBzNa) for piperidinolysis of PS^- at 0.2 mM PS^-, 0.1 M Pip, ≤ 0.06 to > 0.03 M NaOH, 35°C and $[CTABr]_T$/mM = 5 (●), 6 (▲), 7 (■), 10 (○) and 15 (Δ). The dashed lines are drawn through the calculated data points using equation 2 with kinetic parameters (k_0, θ and $K^{X/S}$), listed in Table 1, at $[MX]_0^{op} = 0$. The solid lines are drawn through the calculated data points using equation 2 with kinetic parameters (k_0, θ and $K^{X/S}$), listed in Table 1, at $[MX]_0^{op}$ /mM = 6.3 (●), 6.6 (▲), 6.7 (■), 8.8 (○) and 9.4 (Δ). **Inset**: The plots at magnified scale for the data points at the lowest values of [MX].

Fig. 2. Plots showing the dependence of k_{obs} upon [MX] (MX = 3-BrBzNa) for piperidinolysis of PS^- at 0.2 mM PS^-, 0.1 M Pip, ≤ 0.06 to > 0.03 M NaOH, 35°C and $[CTABr]_T$/mM = 5 (●), 6 (▲), 7 (■), 10 (○) and 15 (Δ). The dashed lines are drawn through the calculated data points using equation 2 with kinetic parameters (k_0, $\theta = F_{X/S}k_{obs}^{MX}$ and $K^{X/S}$), listed in Table 1of SM and Table 1, at $[MX]_0^{op} = 0$. The solid lines are drawn through the calculated data points using eq

2 with kinetic parameters (k_0, $\theta = F_{X/S}k_{obs}^{MX}$ and $K^{X/S}$), listed in Table 1of SM and Table 1, at $[MX]_0^{op}$ /mM = 4.0 (●), 4.1 (▲), 5.7 (■), 6.8 (○) and 15.9 (Δ). **Inset** : The plots at magnified scale for the data points at the lowest values of [MX].

Fig. 3. Plots showing the dependence of shear viscosity (η) upon shear rate (γ) for samples where [PSL] = 0.2 mM, [NaOH] = 0.03 M, [Pip] = 0.1 M, [CTABr] = 15 mM and [2-BrBzNa]/M = 0.02 (♦), 0.04 (■), 0.06 (▲), 0.08 (●), 0.10 (○), 0.20 (Δ), 0.30 (□) and 0.40 (×). **Inset**: The plots of shear viscosity (η) versus shear rate (γ) at magnified scale for the same samples as noted above.

Fig. 4. Plots showing the dependence of shear viscosity (η) upon shear rate (γ) for samples where [PSL] = 0.2 mM, [NaOH] = 0.03 M, [Pip] = 0.1 M, [CTABr] = 15 mM and [4-BrBzNa]/M = 0.005 (×), 0.01 (♦), 0.02 (■), 0.03 (▲), 0.04 (●), 0.05 (○), 0.06 (Δ), 0.08 (□) and 0.1 (◊).

Fig. 5. Plots of shear viscosity at a constant shear rate (i.e. η_γ) versus [MX] for MX = 2-BrBzNa, (▲), 3-BrBzNa, (●) and 4-BrBzNa (○) at $\gamma = 1.0\ s^{-1}$ {**Inset**, MX = 2-BrBzNa, $\gamma = 0.5\ s^{-1}$ (■)}, 15 mM CTABr, 0.2 mM PS^-, 0.03 M NaOH, 0.1 M Pip and ~ 35°C.

Tables

Table 1

Values of the empirical constants θ and $K^{X/S}$, calculated from equation 2 (where $[MX] = [MX]_S^{ef}$ with zero and nonzero $[MX]_0^{op}$ values) for different MX in CTABr micelles[a].

$[CTABr]_T$[b] mM	$10^4 k_o$[c] s^{-1}	$[MX]_o$[op] mM	$10^4 \theta$ s^{-1}	$K^{X/S}$ M^{-1}	$K_{X/S}$ M^{-1}	$F_{X/S}$	$K_{X/S}$[n] M^{-1}	K_X^{Br}[h]	$10^8 \sum di^2$
				MX = 2-$BrC_6H_4CO_2Na$					
5.0	29.3	6.3	206 ± 3.8[d]	9.33 ± 0.49[d]	335.9[e]	0.63[f]	211.6[g]	8.46[h]	84.37
5.0	29.3	0	219 ± 7.8	7.17 ± 0.70	258.1	0.67	172.9	6.92	297.5
6.0	28.8	6.6	199 ± 4.3	8.37 ± 0.50	359.9	0.61	219.5	8.78	92.93
6.0	28.8	0	213 ± 8.6	6.40 ± 0.65	275.2	0.65	178.9	7.16	307.6
7.0	27.7	6.7	199 ± 5.0	7.20 ± 0.48	360	0.61	219.6	8.78	101.6
7.0	27.7	0	213 ± 9.3	5.56 ± 0.58	278	0.65	180.7	7.23	253.9
10.0	26.2	8.8	206 ± 6.3	4.97 ± 0.36	352.9	0.63	222.3	8.89	71.71
10.0	26.2	0	228 ± 13	3.65 ± 0.45	259.2	0.70	181.4	7.26	223.3
15.0	25.8	9.4	212 ± 4.5	3.34 ± 0.15	354	0.65	230.1	9.20	16.75
15.0	25.8	0	241 ± 16	2.41 ± 0.30	255.5	0.74	189.1	7.56	142.4
				MX = 3-$BrC_6H_4CO_2Na$					
5.0	29.8	4.0		51.3 ± 2.7	1847	0.97 ± 0.01	1792	71.7	216.6
5.0	29.8	0		34.8 ± 4.4	1253	1.02 ± 0.04	1291	51.6	1477
6.0	29.2	4.1		46.6 ± 1.0	2004	0.96 ± 0.06	1924	77.0	61.20
6.0	29.2	0		33.4 ± 3.1	1436	1.0 ± 0.03	1436	57.4	1409
7.0	28.5	5.7		42.1 ± 1.7	2105	0.90 ± 0.01	1895	75.8	237.9
7.0	28.5	0		27.3 ± 2.9	1365	0.96 ± 0.03	1310	52.4	1886

10.0	27.5	6.8	27.3 ± 1.1	1938	0.88 ± 0.01	1706	68.2	69.35
10.0	27.5	0	17.7 ± 2.4	1257	0.94 ± 0.04	1182	47.3	944.0
15.0	25.2	15.9	16.8 ± 0.7	1781	0.89 ± 0.01	1585	63.4	133.4
15.0	25.2	0	8.28 ± 1.5	878	1.03 ± 0.08	904.0	36.2	1994
			4- $BrC_6H_4CO_2Na$					
5.0	29.4	3.6	44.6 ± 1.8	1606	0.99 ± 0.01	1590	63.6	321.3
5.0	29.4	0	32.5 ± 2.7	1170	1.04 ± 0.03	1217	48.7	1577
6.0	29.3	4.6	36.6 ± 1.2	1574	0.97 ± 0.01	1527	61.1	171.5
6.0	29.3	0	25.1 ± 2.7	1079	1.04 ± 0.04	1122	44.9	2059
7.0	28.9	5.3	31.7 ± 1.8	1585	0.97 ± 0.02	1537	61.5	528.2
7.0	28.9	0	21.4 ± 1.0	1070	1.06 ± 0.03	1134	45.4	1369
10.0	27.4	10.2	24.7 ± 0.8	1736	0.99 ± 0.01	1736	69.4	123.8
10.0	27.4	0	14.5 ± 1.6	1030	1.09 ± 0.05	1123	44.9	1695
15.0	26.6	14.4	13.2 ± 0.6	1399	0.98 ± 0.02	1371	54.8	192.5
15.0	26.6	0	6.91 ± 1.2	732.5	1.15 ± 0.10	842.4	33.7	2602

[a] [MX] = 2-BrBzNa, 3-BrBzNa and 4-BrBzNa. [b] Total concentration of CTABr. [c] $k_0 = k_{obs}$ at [MX] = 0. [d] Error limits are standard deviation. [e] $K_{X/S} = K^{X/S} (1 + K_S^o [CTABr]_T)$ where $K_S^o = 7000\ M^{-1}$. [f] $F_{X/S} = \theta / k_W$ where $k_W = k_{obs}$ at $[CTABr]_T = 0$, $[Pip]_T = 0.1$ M and the value of k_W, under such conditions is $32.7 \times 10^{-3}\ s^{-1}$ at 35°C. [g] $K_{X/S}^n = F_{X/S} K_{X/S}$. [h] $K_X^{Br} = K_{X/S}^n / K_{Br/S}^n$, where $K_{Br/S}^n = 25\ M^{-1}$.

Table 2

The mean values of $F_{X/S}$ and K_X^{Br} for different MX in the presence of CTABr micelles[a].

X	$[MX]_o^{op}$	$10^2 F_{X/S}$	K_X^{Br}	$[MX]_{sc}$[b] mM
2-$BrC_6H_4CO_2^-$	nonzero	63 ± 2[c]	8.8 ± 0.3[c]	-
(2-$BrBz^-$)	zero	68 ± 4	7.2 ± 0.2	
3-$BrC_6H_4CO_2^-$	nonzero	92 ± 4	71 ± 6	50
(3-$BrBz^-$)	zero	99 ± 4	49 ± 8	
4-$BrC_6H_4CO_2^-$	nonzero	98 ± 1	62 ± 5	50
(4-$BrBz^-$)	zero	108 ± 5	44 ± 6	
3-$FC_6H_4CO_2^-$	nonzero	71 ± 6	12.8 ± 0.9[d]	70,70
4-$FC_6H_4CO_2^-$	nonzero	80 ± 2	13.4 ± 0.6[d]	70,80
$C_6H_5CO_2^-$ (Bz^-)	zero	70	5.8[e]	
2-$ClBz^-$		-	4.0[f]	
3-$ClBz^-$	nonzero	72	50[g]	
2,6-Cl_2Bz^-	-		5.0[h]	
2-CH_3Bz^-	nonzero	43	4.9[i]	
3-CH_3Bz^-	nonzero	50	17.7[i]	
4-CH_3Bz^-	nonzero	48	16.7[i]	

[a] Unless otherwise noted cationic micelles are CTABr. [b] The specific concentration of MX for the occurrence of the viscosity maximum of the plot of η versus [MX] at 15 mM CTABr. [c] Error limits are standard deviations. [d] Ref. [19]. [e] Ref. [38]. [f] Ref. [39]. [g] Ref. [40]. [h] Ref. [4]. [i] The values of K_X^{Br} were recalculated from the observed data published as Ref. [18].

For Table of contents use only

Kinetic and rheological measurements of the effects of inert 2-, 3- and 4-bromobenzoate ions on the cationic micellar-mediated rate of piperidinolysis of ionized phenyl salicylate.

Nor Saadah M. Yusof and M. Niyaz Khan[*]
Department of Chemistry, Faculty of Science, University of Malaya, 50603 Kuala Lumpur, Malaysia

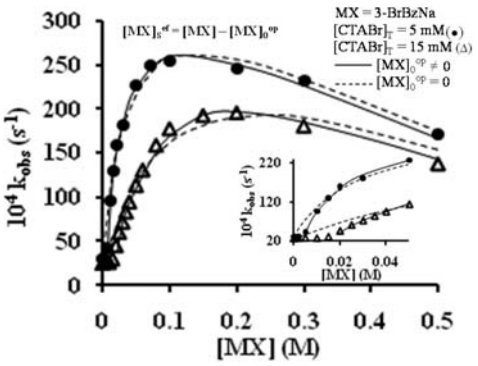

Kinetic observation of the effects of [3-BrBzNa] on the rate of piperidinolysis of ionized phenyl salicylate in the presence of CTABr micelles.

Research Highlights

- Determination of ion exchange constants, K_X^{Br}, for counterions of cationic micelles
- New kinetic model is used to study the effects of inert salts, MX, on cationic micellar mediated reaction rates
- Relationship between magnitudes of K_X^{Br} and formation of wormlike micelles
- Kinetic demonstration of the occurrence of independent ion exchange processes on micelle
- Plots of shear viscosity *vs* [MX] exhibit maxima – indicative of wormlike micelles